

The reaction of hydroxylamine with aspirin

Michelle Medeiros,^a Bruno S. Souza,^a Elisa S. Orth,^a Tiago A. S. Brandão,^b
Willian Rocha,^b Anthony J. Kirby,^{c*} and Faruk Nome^{a*}

^aINCT-Catálise, Departamento de Química, Universidade Federal de Santa Catarina,
Florianópolis, SC, 88040-900, Brazil

^bDepartamento de Química, Universidade Federal de Minas Gerais, Belo Horizonte, Minas
Gerais, 31270-901, Brazil. ^c University Chemical Laboratory, Cambridge CB2 1EW, UK
E-mail: ajkl@cam.ac.uk, faruk@gmc.ufsc.br

We dedicate this paper to Rita H. de Rossi, in recognition of her many distinguished
contributions to Physical Organic Chemistry

DOI: <http://dx.doi.org/10.3998/ark.5550190.0012.738>

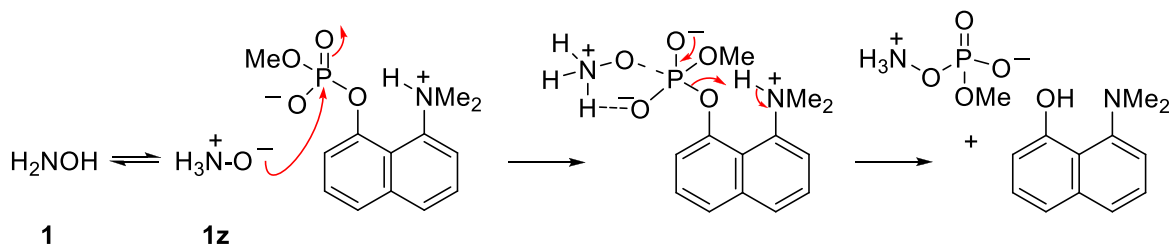
Abstract

Hydroxylamine reacts with aspirin in aqueous solution at 25 °C predominantly through oxygen, to give *O*-acetylhydroxylamine as the initial product (Scheme 3). The reaction is much faster than the intramolecular general base catalysed hydrolysis of the carboxylate anion, as it is also for the CO₂H form of aspirin. Both reactions are faster than expected, consistent with moderate activation and/or proton transfer catalysis of hydroxylaminolysis by both CO₂⁻ and CO₂H groups. Calculations support oxygen attack as the preferred reaction, but do not permit a clear choice between mechanisms involving NH₂OH and ⁺NH₃-O⁻ as the effective nucleophile.

Keywords: Ester hydrolysis, hydroxylamine, ammonia oxide, alpha-effect, Jaffé plot

Introduction

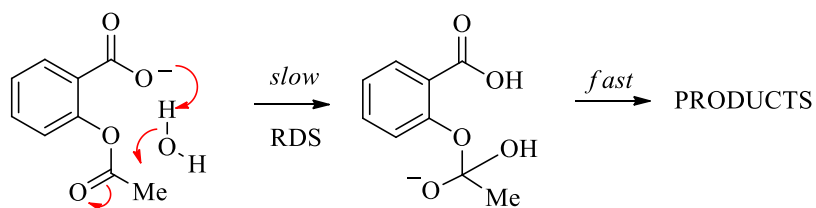
Reactions involving nucleophilic attack by hydroxylamine are of special interest because of its remarkably high reactivity in nucleophilic substitutions at carboxylic acyl and phosphoryl centers: which has been accounted for in terms of a unique ambident α -nucleophilicity. A α -effect nucleophile is identified by the presence of a lone pair of electrons on the atom adjacent to the nucleophilic center: but hydroxylamine is also an ambident nucleophile – alkylated on nitrogen, but typically acylated and phosphorylated on oxygen.¹ Thus in reactions with methyl 8-dimethylamino-1-naphthyl phosphate, hydroxylamine and its *N*-methylated derivatives show similar high reactivity, but reactions with *O*-methylated derivatives are significantly slower. It is proposed that the reactions of NH₂OH on oxygen involve pre-equilibrium formation of the zwitterionic tautomer ammonia oxide, ⁺H₃N-O⁻, as the active nucleophile (Scheme 1).²

**Scheme 1**

The mechanism of nucleophilic attack by hydroxylamine has been discussed extensively over the years. Jencks identified *O*-acylhydroxylamine derivatives as the major initial products in reactions of hydroxylamine with a number of acylating agents, and was the first to attribute the high reactivity to the zwitterionic form of hydroxylamine.³ However, *alkylation* of hydroxylamine occurs on nitrogen rather than on oxygen, and the high acylation reactivity of oxygen could involve intramolecular general acid-base catalysis: which would not be feasible in the concerted linear displacements involved in alkylation.¹

We have recently shown, using computation and crystallography, that the zwitterionic tautomer **1z** is the preferred form of hydroxylamine in the crystal of its half-hydrochloride $(\text{NH}_2\text{OH})_2\cdot\text{HCl}$. Although **1z** (Scheme 1) is not an α -effect nucleophile as usually defined, it is well suited to substitution reactions involving addition-intermediates, because proton transfer from the H_3N^+ group to a developing negatively charged center, *e.g.*, the oxygen of a $\text{C}=\text{O}$ or $\text{P}=\text{O}$ group in the substrate, becomes thermodynamically favorable as reaction proceeds (Scheme 1).⁴

Proton transfer catalysis is important in many substitution reactions, contributing significant rate enhancements. A classical example is the hydrolysis of the aspirin (acetyl salicylic acid) monoanion, for which water attack is facilitated by intramolecular general base catalysis by the carboxylate group (Scheme 2).⁵

**Scheme 2**

We report a study of the reactions of hydroxylamine with substituted aspirins, designed to identify the reactive nucleophile(s) involved – and possible further interesting mechanistic variations. We present new evidence consistent with the dominant nucleophilic contribution of

the zwitterionic form of hydroxylamine, in competition with a reaction where intramolecular proton transfer is of fundamental importance.

Results and Discussion

Reaction with hydroxylamine

Reactions of hydroxylamine with substituted aspirins were investigated at pH 6.00, where only the anionic form of the substrate is present: the k_{obs} values obtained are plotted in Figure 1 as a function of neutral $[\text{NH}_2\text{OH}]$ concentration. The experimental points in Figure 1 were fitted to Equation 1, where k_0 is the rate constant for the spontaneous hydrolysis and k_{N_2} is the second-order rate constant for reaction of a substituted aspirin with neutral hydroxylamine. Derived second-order rate constants are given in Table 1, together with available literature k_0 values.

$$k_{\text{obs}} = k_0 + k_{\text{N}_2}[\text{NH}_2\text{OH}] \quad (1)$$

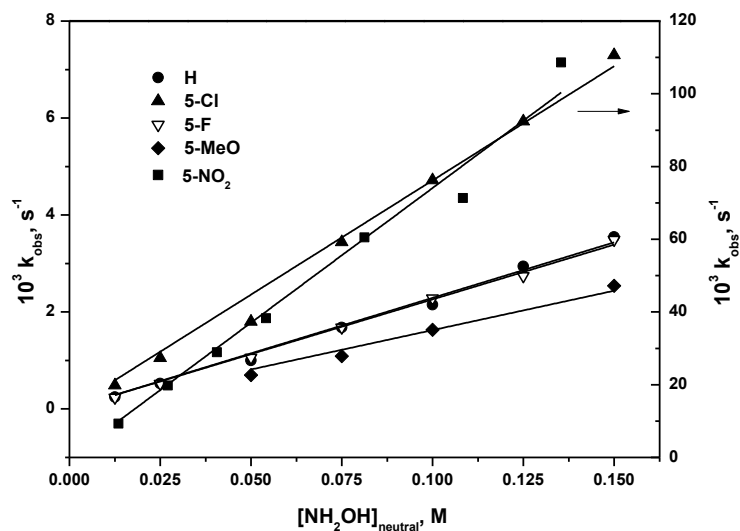


Figure 1. Plot of k_{obs} as a function of neutral hydroxylamine concentration for reactions with substituted aspirins at 25.0 °C, pH = 6.00 and $\mu = 1.0$ M (KCl). (Data for the 5-NO₂ compound follow the right hand scale.) The concentration of free hydroxylamine was calculated based on $\text{p}K_{\text{a}} = 6.0$. Data are given in Table S1 in the Supporting Information.

Table 1. Values of k_0 and k_{N_2} for the reactions of hydroxylamine and substituted aspirins, pH = 6.0, 25.0 °C and $\mu = 1.0$ M (KCl)

Aspirin	$10^6 k_0, \text{s}^{-1}{}^a$	$10^2 k_{\text{N}_2}, \text{M}^{-1} \text{s}^{-1}$
5-MeO	2.20	1.62
H	2.64	2.29

Table 1. Continued

Aspirin	$10^6 k_o, s^{-1}$ ^a	$10^2 k_{N2}, M^{-1} s^{-1}$
5-F	2.64	2.26
5-Cl	2.86	4.71
5-NO ₂	5.57	80.2

^aData from the literature, estimated for 25° using $E_a = 18.95 \text{ kcal mol}^{-1}$ as measured for AAS^{-5,6}

The rate of cleavage of aspirin is enhanced up to 10^4 -fold in the presence of 0.3 M hydroxylamine, an indication of the magnitude of the apparent α -effect: this factor depends on the aspirin substituent, as discussed below.

The pH-dependence of the reaction was also evaluated: reactions of hydroxylamine with substituted aspirins were followed over the pH range 2-9, at 25 °C and ionic strength $\mu = 1.0 \text{ M}$ (KCl) in buffered solutions containing 0.3 M hydroxylamine. The kinetic results are shown in Figure 2 and the parameters obtained by fitting the data with Equation 2 are given in Table 2. Equation 2 is derived from Scheme 3, which summarises the possible reactions of substituted aspirins and their anions with water and hydroxylamine. In Equation 2, k_{W1} and k_{W2} correspond, respectively, to the spontaneous hydrolyses of protonated (χ_{AASH}) and anionic (χ_{AAS^-}) aspirin and k_{N1} and k_{N2} correspond to reactions of neutral hydroxylamine with nonionic and anionic aspirin, respectively.

As shown in Table 2, the rate constants for the reaction of the anionic form of the aspirin derivatives with hydroxylamine are in all cases at least 10^4 times greater than the rate constants determined for the hydrolysis reaction.⁶ Thus, under the conditions used, a reaction path involving the addition of a water molecule can be ruled out.

$$k_{obs} = (k_{W1} + k_{N1}[\text{NH}_2\text{OH}]_{total} \cdot \chi_{\text{NH}_2\text{OH}}) \cdot \chi_{\text{AASH}} + (k_{W2} + k_{N2}[\text{NH}_2\text{OH}]_{total} \cdot \chi_{\text{NH}_2\text{OH}}) \cdot \chi_{\text{AAS}^-} \quad (2)$$

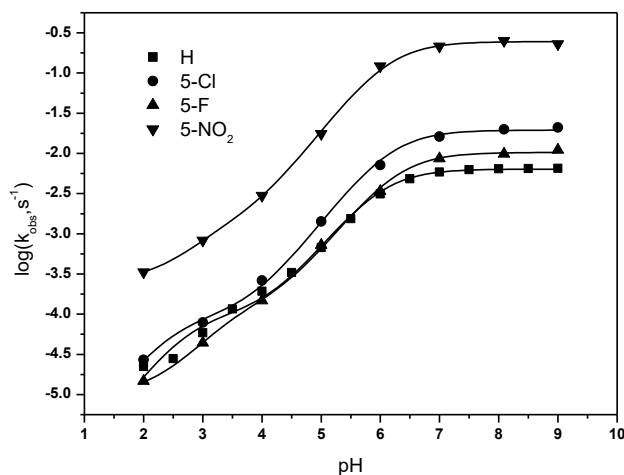
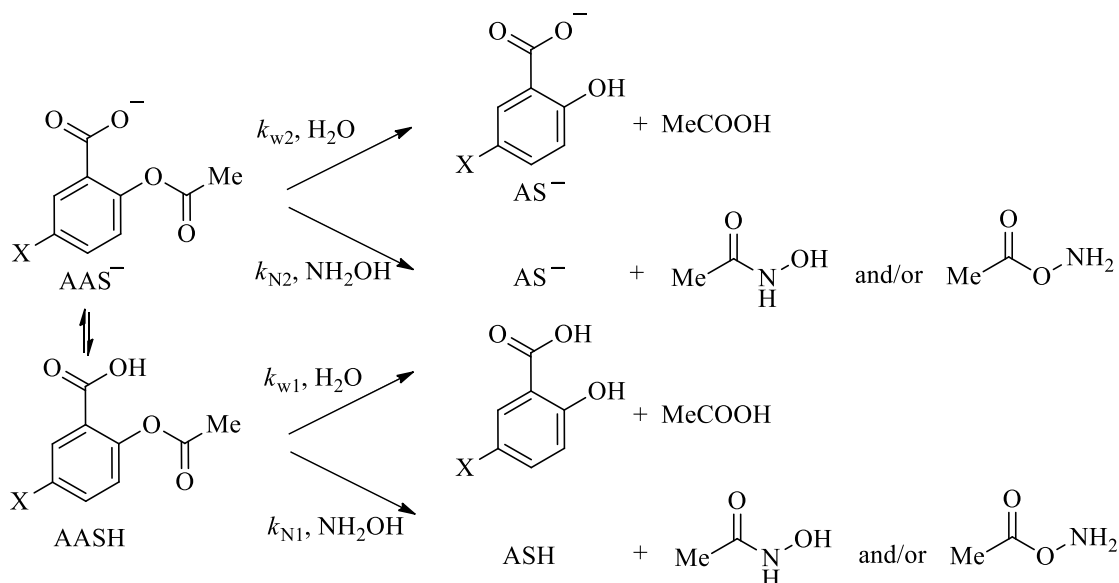


Figure 2. pH Rate profiles for reactions of substituted aspirins with 0.3 M hydroxylamine at 25.0 °C and $\mu = 1.0$ M (KCl). The data were fitted to Equation 2 using the kinetic parameters shown in Table 2. Full data are given in Table S2 in the Supporting Information.



Scheme 3

The pH-rate profiles for reactions of substituted aspirins with hydroxylamine (Figure 2) show the rate increases with pH expected from deprotonation of the NH_3^+ group of the nucleophile, reaching a plateau above pH 7-8, where hydroxylamine is fully converted to the free base.

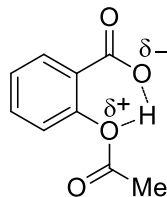
Table 2. Values of k_{N1} and k_{N2} from fits of pH-rate profiles for reactions of hydroxylamine with substituted aspirins (Scheme 3). Rate constants are within 5% error

AAS, X =	pK_a	$10^1 k_{N1}, \text{M}^{-1} \text{s}^{-1}$	$10^2 k_{N2}, \text{M}^{-1} \text{s}^{-1}$	$10^6 k_{w2}, \text{s}^{-1} \text{ }^{a,b}$
H	3.38 ^c	2.65	2.18	2.64
5-F	3.24 ^d	1.13	3.30	2.64
5-Cl	3.21 ^d	14.4	6.51	2.86
5-NO ₂	2.78 ^d	32.6	82.8	5.57

^aData from Table 1. ^bValues of k_{w1} are at least an order of magnitude smaller. ^cData from the literature.⁷ ^dValues determined by potentiometric titration at $\mu = 0$.

Although the observed rate constants increase with increasing pH (Figure 2), the reactions of hydroxylamine with the CO_2H form of the substituted aspirins (k_{N1}) are faster than those (k_{N2}) for reactions with anionic forms (Table 2). As suggested in Scheme 4, the ester carbonyl group of

neutral aspirin can be activated, and the leaving group stabilized, by intramolecular proton transfer from the carboxylic acid moiety. Similar, stronger interactions in the transition state define the intramolecular general acid catalysis mechanism favored by St. Pierre and Jencks.⁷



Scheme 4

The k_{N2} values are also at least one order of magnitude larger than values for reactions with comparable phenyl acetates:⁷ unexpectedly, because charge screening and the electronic effect of the CO_2^- group ($\sigma_m = -0.10$ ⁸) should disfavor nucleophilic attack (but see St. Pierre and Jencks⁷). There appears to be a small but significant electronic (because observed also for *p*-carboxyphenyl acetate⁷) effect of CO_2^- that accelerates attack of hydroxylamine.

Solvent kinetic isotope effect (kie). The reactions were followed at 25.0 °C in the presence of 0.15 M $[NH_2OH]$ in H_2O and D_2O at $pH(D)$ 8.50; i.e. in the plateau region in the pH -rate profile, where both nucleophile and aspirin derivatives are deprotonated. The solvent kinetic isotope effects, k_{H_2O}/k_{D_2O} , of 1.35-1.75 (Table 3), are consistent with nucleophilic attack by hydroxylamine, assisted by intramolecular general base catalysis by the carboxylate group. Similar values have been consistently observed for reactions involving nucleophilic attack with proton transfer in the transition state (TS): *e.g.*, for the reaction of hydroxylamine with 8-dimethylammonium-naphthyl-1-phosphate monoester, where the solvent deuterium isotope effect is 1.67.⁹

Table 3. Solvent isotope effects (k_{H_2O}/k_{D_2O}) for reactions of hydroxylamine with substituted aspirins at 25.0 °C, $[NH_2OH] = 0.15$ M, $pH(D) = 8.5$ and $\mu = 1.0$ M (KCl)

Aspirin	k_{H_2O} / k_{D_2O}
H	1.75 ± 0.09
5-F	1.70 ± 0.08
5-Cl	1.68 ± 0.12
5-NO ₂	1.35 ± 0.15

***N*-Acetylhydroxylamine** concentrations were measured colorimetrically, *via* complexation with Fe(III), using a modification of the method of Lipmann and Tuttle.¹⁰ Yields of *N*-acetylhydroxylamine were $25 \pm 5\%$ for all the substituted aspirins, with the exception of the 5-nitro derivative (found: 55%), for experimental details see Supporting Information. Previous

studies^{3,11} show that *O*-acetylhydroxylamine isomerises to *N*-acetylhydroxylamine, at a rate which depends on the concentration of hydroxylamine and on the pH of the medium. Under the conditions used for the quantification of *N*-acetylhydroxylamine, at pH 8.50 and $[\text{NH}_2\text{OH}] = 0.05\text{M}$, the rate constant for the conversion can be estimated to be of the order of $1.2 \times 10^{-4} \text{ s}^{-1}$, giving a half life of approximately 90 min. For the quantification experiments the reactions were followed for 1 h for H-AAS and 5-F AAS: for 30 min for 5-Cl AAS, for 80 min for 5-MeO AAS and for 2 min for 5-NO₂ AAS. Thus some of the *N*-acetyl-hydroxylamine measured must come from the isomerisation of *O*-acylhydroxylamine rather than directly from the reaction with the aspirin. The limited amounts *N*-acetylhydroxylamine formed show that the reactions of aspirins with hydroxylamine occur primarily *via* the attack of the oxygen atom on the ester carbonyl, forming *O*-acetylhydroxylamine as the major initial product (at least 75%, except for 5-NO₂ AAS): consistent with the original results of Jencks.³ We have carried out a computational investigation to establish which reaction pathway is more favorable: see below.

Jaffé plot. Substituent effects on reactions of hydroxylamine with substituted aspirins were examined by fitting results to Equation 3, which considers the interactions of the OAc group and the carboxylate ion with substituent groups to be independent. Thus a methoxy group should increase the basicity of CO₂⁻, but decrease the electrophilicity of the ester C=O group, with opposite effects on the reaction rate. These effects can be assessed separately by using the Jaffé equation (Equation 3),¹² where ρ_{acid} is related to the effect on the carboxylate group and ρ_{phenol} is related to that on the ester group. The Jaffé plot (Figure 3) is based on the data in Table 4.

$$\log(k_X/k_H) = \rho_{\text{acid}}\sigma_{\text{meta}} + \rho_{\text{phenol}}\sigma_{\text{para}} \quad (3)$$

Table 4. Rate constants and parameters used for the Jaffé plot

Aspirin	$10^2 k_{\text{N}_2}, \text{M}^{-1} \text{s}^{-1}$	$\log(k_X/k_H)$	σ_{m}^*	σ_{p}^*
5-MeO	1.62	-0.21	0.11	-0.26
H	2.29	-	-	-
5-F	2.26	-0.068	0.34	-0.03
5-Cl	4.71	0.25	0.37	0.19
5-NO ₂	80.2	1.48	0.72	1.24

* σ values are from Williams.⁸

The derived value of 1.46 for ρ_{phenol} indicates a TS where the C–O bond is approximately 65% broken (calculated using the effective charge index⁸): while the value of -0.81 for ρ_{acid} indicates a substantial decrease in the negative charge of the carboxylate group, consistent with it acting as an intramolecular general base. The Jaffé parameters are thus consistent with a more or less concerted mechanism, with simultaneous bond formation between the oxygen atom and the carbonyl group and bond breaking between the leaving group and carbonyl center in the TS,

rather than formation of a discrete tetrahedral addition intermediate, as proposed for aspirin hydrolysis.⁵

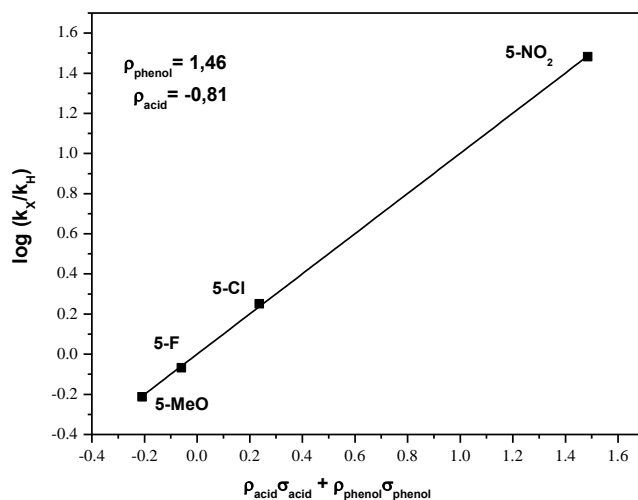


Figure 3. Jaffé plot for reactions of hydroxylamine with substituted aspirins. σ_{acid} and σ_{phenol} are defined as σ_m or σ_p depending on the relative positions of group and substituent.

Calculations and proposed mechanisms. Since hydroxylamine is an ambident α -nucleophile, equilibrating in solution between NH_2OH and the zwitterionic $^+\text{H}_3\text{N}-\text{O}^-$ form, we have analyzed three different, kinetically indistinguishable, modes of attack of hydroxylamine on the aspirin anion AAS^- (Scheme 3) which could, in principle, account for the KIE observed. In the gas phase, three TS structures were located: **TS-NH₂**, **TS-OH** and **TS-O⁻** (Figure 4). The first two structures correspond to the attack of neutral NH_2OH on AAS^- by the NH_2 and OH groups, respectively, and the last corresponds to the attack of $^+\text{H}_3\text{N}-\text{O}^-$. In each of the three TS structures found, the imaginary frequency corresponds to the proton transfer from the nucleophile to the CO_2^- group concerted with attack by N (in **TS-NH₂**) or O4 (in **TS-OH** and **TS-O⁻**) on C2. Besides the transition states and reactants, no other stable minimum (intermediate) could be found in any of the calculations. Selected structural details of the transition state structures are given in Table 5, along with those of salicylic acid (**AS⁻**), acetohydroxamic acid (**Nacet**), *O*-acetylhydroxylamine (**Oacet**), hydroxylamine (**NH₂OH**) and the hydroxylamine zwitterion ($^+\text{NH}_3-\text{O}^-$). Structural details of reactants and products are included in the electronic supporting information.

As shown in Table 5, the extent of proton transfer and bond formation between the nucleophilic and electrophilic centers varies significantly depending on the mode of attack of hydroxylamine. A better understanding of the main structural changes and energy variations along the reaction coordinate can be obtained from IRC calculations in the reverse and forward directions, starting from the three transition states found. These results are shown in Figure 5.

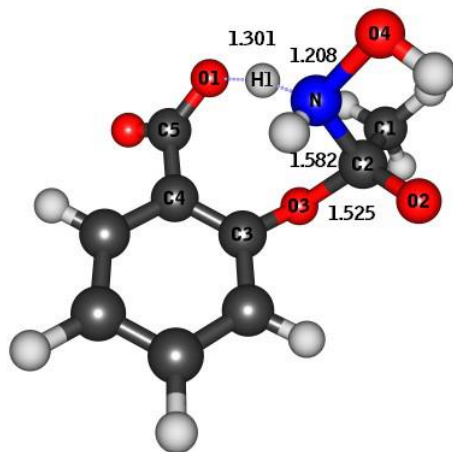
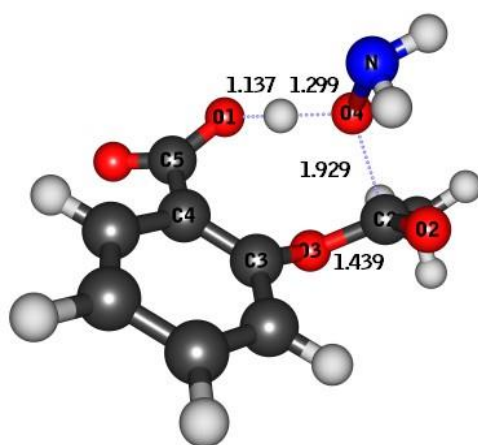
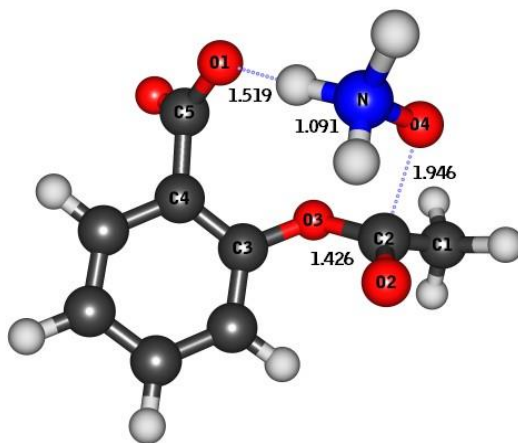
**TS-NH₂****TS-OH****TS-O⁻**

Figure 4. B3LYP/6-31+g(d) transition state structures for the attack of neutral hydroxylamine through its NH₂ and OH groups (TS-NH₂ and TS-OH, respectively) and for the attack of ⁺H₃N-O⁻ (TS-O⁻) on AAS⁻.

Table 5. Main geometrical parameters of **TS-NH₂**, **TS-OH**, **TS-O⁻**, **AAS⁻**, **AS⁻**, **NAcet** and **OAcet** calculated at the B3LYP/6-31+g(d) level. Bond lengths are given in Å and the dihedral angle is given in degrees

	O1-H	N-H	O4-H	C2-N	C2-O4	C2-O3	C2-O2	C2-O3-C1-O2
TS-NH ₂	1.301	1.208	-	1.582	-	1.525	1.278	23.520
TS-OH	1.137	-	1.299	-	1.929	1.439	1.234	15.438
TS-O ⁻	1.519	1.091	-	-	1.946	1.426	1.239	14.385
AAS ⁻	-	-	-	-	-	1.370	1.211	1.904
AS ⁻	1.037	-	-	-	-	-	-	-
NAcet	-	-	-	1.367	-	-	-	-
OAcet	-	-	-	-	1.355	-	-	-
NH ₂ OH	-	1.022	0.970	-	-	-	-	-
⁺ NH ₃ O ⁻	-	1.036	-	-	-	-	-	-

TS-NH₂ shows bond formation between **NH₂OH** and **AAS⁻** further developed than in **TS-O⁻** or **TS-OH**, with a C2-N bond-length of 1.582 Å, only 0.215 Å longer than in the product **NAcet**. As shown in Figs. 4 and 5A, there is also effective intramolecular proton transfer from the developing H₂N⁺ of **NH₂OH** to the neighboring carboxylate oxygen O1, with N-H1 and O1-H1 distances changing from 1.208 Å and 1.301 Å in **TS-NH₂** to 1.298 Å and 1.201 Å at S = 0.2, respectively. This proton transfer is concerted with leaving group departure, which is further advanced than in **TS-OH**, with C2-O3 = 1.525 Å and C2-O3-C1-O2 equal to 23.52°. As observed for both **TS-O⁻** and **TS-OH**, the C2-O2 (C=O) bond length remains almost unchanged, consistent with a concerted TS, without formation of a tetrahedral intermediate structure.

The transition state structure **TS-OH**, corresponding to the attack of neutral hydroxylamine on **AAS⁻** through its OH group, shows proton transfer far advanced at S = 0, with an O1-H1 bond-length of 1.137 Å and O4-H1 = 1.299 Å, corresponding to intramolecular general base catalysis by the substrate carboxylate group. As observed also for the attack of ⁺H₃N-O⁻, the extent of bond formation between C2-O4 is small at S = 0, and this bond length decreases before effective proton transfer takes place (Figure 5B); which occurs slightly before S = 0. The C2-O2 bond remains almost unchanged in **TS-OH** (see Table 5), while the carbonyl carbon is considerably out-of-plane, with C2-O3-C1-O2 = 15.44°. The C2-O4 bond distances are very similar in **TS-OH** and **TS-O⁻**, although in the latter case the original H1 is transferred to the CO₂⁻ moiety only at S > 2.40Å.

In **TS-O⁻** there is a very small amount of proton transfer from the ⁺NH₃ group to CO₂⁻, the N-H1 bond length increasing from 1.036 in ⁺NH₃-O⁻ to 1.091 Å. There is also only a small amount of bond formation between the C2-O4 atoms, which distorts the angle C2-O3-C1-O2 from 1.90° in **AAS⁻** to 14.38° in **TS-O⁻**. As shown in Figure 5C, the proton is effectively transferred only at S > 2.50Å, while C2-O4 bond formation starts before S = 0. The C2-O3 bond-length increases with the approach of the nucleophile whereas C2-O2 remains almost constant along the reaction coordinate, varying from 1.211 Å in **AAS⁻** to 1.239 Å in **TS-O⁻** and 1.216 Å in **OAcet** (Table 5).

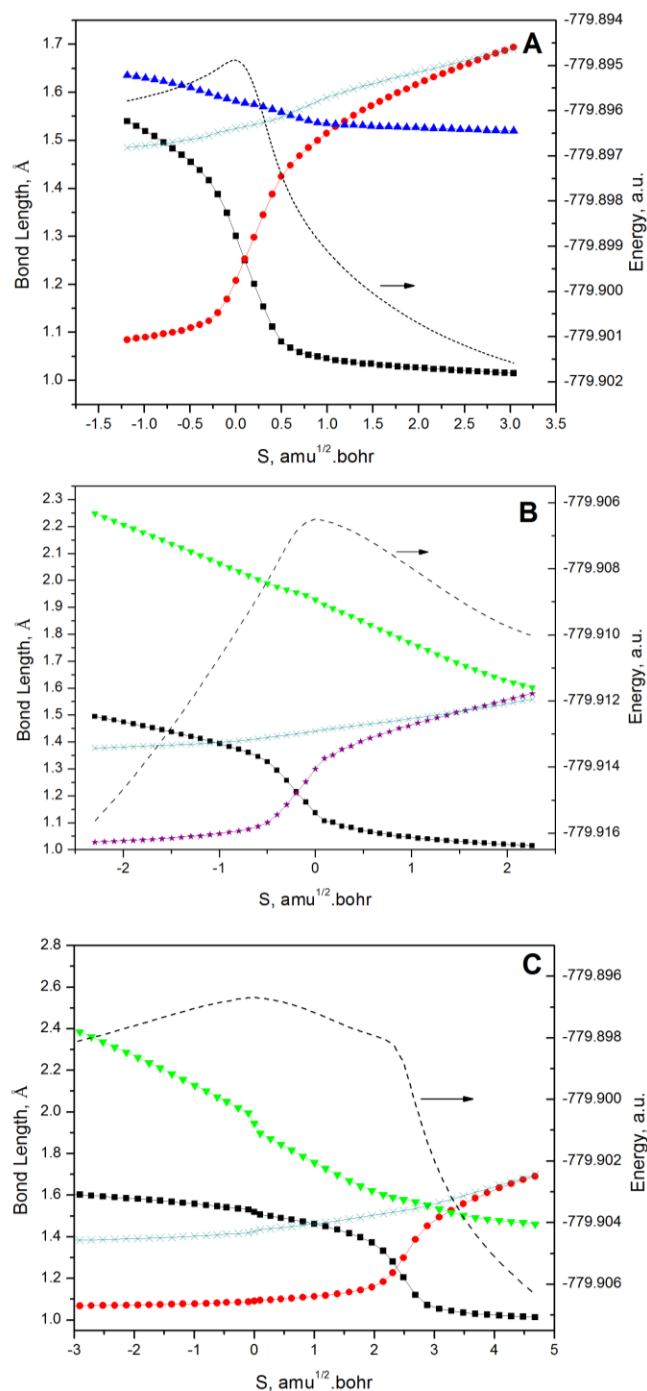


Figure 5. –Intrinsic reaction coordinates (IRC) computed at the B3LYP/6-31+G(d) level for the nucleophilic attack of neutral hydroxylamine through NH_2 (A) and OH (B) and for the attack of $^+\text{H}_3\text{N}-\text{O}^-$ (C) on AAS^- showing the variation of O1-H (■), N-H (●), O4-H1 (★), C2-O3 (×), C2-O4 (▼) and N-C2 (▲) bonds. The energy variation is given by the dashed line. The $S = 0$ coordinates correspond to **TS-NH₂** (A), **TS-OH** (B) and **TS-O⁻** (C), shown in Figure 4.

The small amount of bond formation between the nucleophile and the carbonyl carbon in **TS-O⁻**, with C2-O4 bond equal to 1.946 Å compared to 1.355 Å in **OAcet**, indicates that **TS-O⁻** is an early transition state, with neither proton transfer or bond formation well developed.

Computed relative energies, obtained at the MP4(SDQ)/6-31+g(d)//B3LYP/6-31+g(d) level, with solvation effects included, of all species along the reaction coordinate are shown in Figure 6, where the sum of the reactant energies at infinite separation is taken as the reference point. Starting from **AAS⁻** and neutral **NH₂OH** there are high energy barriers corresponding to $\Delta G_{(sol)}^\ddagger$ of 19.64, 20.2 and 24.52 kcal.mol⁻¹ for **TS-O⁻**, **TS-OH** and **TS-NH₂**, respectively. Clearly, the attack of hydroxylamine through oxygen, in both neutral and the zwitterionic forms, involves smaller barriers than **TS-NH₂**, by 4.30 and 4.88 kcal.mol⁻¹ for **TS-OH** and **TS-O⁻**, respectively, in agreement with the experimental observation of the predominant formation of **OAcet**. The activation energies calculated for the attack of hydroxylamine through oxygen are very close for the neutral and zwitterionic forms, and in excellent agreement with the experimental value of 19.6 kcal.mol⁻¹ (for details see Supporting Information). Results obtained using the B3LYP electronic energies are very similar to those obtained using Equation 4, giving $\Delta G_{(sol)}^\ddagger$ for **TS-O⁻**, **TS-OH** and **TS-NH₂** of 19.26, 19.63 and 26.21 kcal.mol⁻¹. Thus, the theoretical results indicate, correctly, that hydroxylamine attacks **AAS⁻** exclusively through oxygen. Since proton transfer takes place with closely similar $\Delta G_{(sol)}^\ddagger$ values in both **TS-O⁻** and **TS-OH**, it is not possible to identify the reactive species unambiguously as the neutral or zwitterionic form of hydroxylamine.

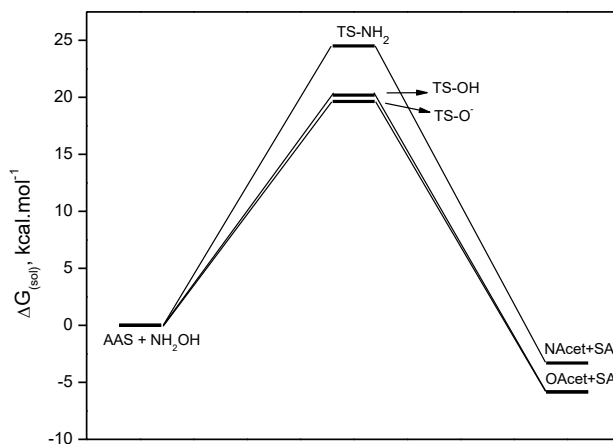


Figure 6. – Free energy variation for the nucleophilic attack of hydroxylamine on **AAS⁻** obtained at the MP4(SDQ)/6-31+g(d)//B3LYP/6-31+g(d) according to Equation 4.

Conclusions

The reaction of hydroxylamine with aspirin in aqueous solution at 25 °C involves predominant reaction through oxygen, to give *O*-acetylhydroxylamine (Scheme 3). This isomerizes moderately rapidly to *N*-acetylhydroxylamine under the conditions. The reaction is overwhelmingly faster than the intramolecular general base catalysed hydrolysis for the carboxylate anion, as it is also for the CO₂H form of aspirin. Both reactions are also faster than expected for the attack of hydroxylamine on phenyl acetate, consistent with moderate activation and/or proton transfer catalysis of hydroxylaminolysis by both CO₂H and CO₂⁻ groups. Calculations support oxygen attack as the preferred reaction, but do not permit a clear choice between mechanisms involving NH₂OH and ⁺NH₃-O⁻ as the effective nucleophile.

Experimental Section

General. Hydrochloride salts of NH₂OH were obtained from Aldrich. Solutions were prepared immediately before use. All measurements were at 25 °C. Inorganic salts were of analytical grade and were used without further purification. Liquid reagents were purified by distillation.

Synthesis of substituted aspirins

Substituted aspirins were prepared according to the procedure of Broxton *et al.*,¹³ and identified by ¹H NMR and melting point.

Kinetics and product identification

Reactions were followed spectrophotometrically by monitoring signals of the salicylates at 297-319 nm, on an HP 8453 UV/Vis diode-array spectrophotometer, with a thermostatted cell holder, in aqueous solutions and under first order conditions. The ionic strength was 1.0 M (KCl) and pH was controlled with 0.01 M ClCH₂CO₂H (pH 2.00-3.00), CH₃CO₂H (pH 4.00-5.00) and TRIS (pH 8.00-9.00) buffers. Solutions at pH 6.00-7.00 were self-buffered by hydroxylamine. pH measurements were with a Metrohm model 713 pH meter. For reactions in D₂O pD = pH_{read} + 0.4.¹⁴ Reactions were started by adding 20 μL of an acetonitrile stock solution of the substrate to 3 mL of reaction mixture and substrate concentration in the cuvette was 1.33 × 10⁻⁴ M, except for 5-nitro-aspirin, where it was 6.67 × 10⁻⁵ M. All reactions were followed for at least four half-lives and observed first-order rate constants, *k*_{obs}, were calculated from linear plots of ln(A_∞-A₀) against time; correlation coefficients were > 0.999. Second-order rate constants were calculated from plots of *k*_{obs} against [nucleophile]. The salicylates were identified by comparing the final kinetic spectrum with the spectra of standard samples at the same pH. The percentage of attack of hydroxylamine *via* oxygen or nitrogen atom was evaluated monitoring *N*-Acetylhydroxylamine as the Fe(III) complex by a modification of the procedure of Lipmann and Tuttle.¹⁰

Calculations and proposed mechanisms

Full geometry optimizations and frequency calculations were performed at the gradient-corrected DFT level,¹⁵ using the hybrid functional formed by the three parameter fit of the exchange-correlation potential B3, suggested by Becke,¹⁶ in conjunction with the correlation functional suggested by Lee *et al.*¹⁷

All atoms were treated with the all-electron split valence 6-31+G(d) basis set,^{18,19} which includes a set of five polarization functions on the C, N and O atoms, with exponential coefficients $\alpha = 0.8$, respectively, and also diffuse functions²⁰ on these elements. The stationary points located on the gas phase potential energy surface were characterized by calculating the Hessian matrices at the B3LYP level, where the minimum energy structures have no imaginary frequency and the transition-state structures have one imaginary frequency. The transition state structures obtained on the potential energy surface for nucleophilic attack of hydroxylamine towards **AAS**⁻ were located using the quadratic synchronous approach of Schlegel and co-workers,²⁰ starting with a low level computed Hessian matrix for a suitable guess transition state structure. To obtain deeper insight into the reaction mechanism, we calculated the intrinsic reaction coordinate (IRC)²¹ using the Gonzalez-Schlegel second-order path,^{22,23} starting from the optimized transition-state structures, with a step length of 0.100 (a.m.u.)^{1/2}.Bohr. Aiming to obtain better energetic results, single-point energy calculations on the B3LYP optimized geometries were performed at the fourth order Møller-Plesset perturbation theory with single, double, and quadruple excitations, MP4(SDQ), using the same basis set. Solvent effects ($G_{\text{solvation}}$) were included by means of the polarizable continuum Model (PCM)²⁴ in single point calculations, with the molecular cavity computed, explicitly including hydrogen, using the UFF radius.²⁵ Thermal corrections to Gibbs free energy (G_{therm}), were estimated at $T = 298.15$ K and $p = 1$ atm using the rigid rotator-harmonic oscillator approximation²⁶ at the B3LYP/6-31+G(d) level in vacuum. The Gibbs free energies of all species in solution were obtained using Equation 4, where $G_{\text{solvation}}$ and G_{therm} were obtained at the B3LYP/6-31+g(d) level and are defined above; E_{MP4} is the electronic energy computed in single point calculations at the MP4(SDQ)/6-31+g(d) level.

$$G_{(\text{sol})} = E_{\text{MP4}} + G_{\text{solvation}} + G_{\text{therm}} \quad (4)$$

All calculations reported here were performed using the Gaussian03 program.²⁷

Acknowledgements

We are grateful to INCT-Catálise, CNPq, Capes, PRONEX and FAPESC for support of this work.

References

1. Jencks, W. P. *Catalysis in Chemistry and Enzymology*; Dover Publications, Inc.: New York, 1969.
2. Kirby, A. J.; Lima, M. F.; da Silva, D.; Roussev, C. D.; Nome, F. *J. Am. Chem. Soc.* **2006**, *128*, 16944.
3. Jencks, W. P. *J. Am. Chem. Soc.* **1958**, *80*, 4581.
4. Kirby, A. J.; Davies, J. E.; Brandao, T. A. S.; da Silva, P. F.; Rocha, W. R.; Nome, F. *J. Am. Chem. Soc.* **2006**, *128*, 12374.
5. Fersht, A. R.; Kirby, A. J. *J. Am. Chem. Soc.* **1967**, *89*, 4857.
6. Fersht, A. R.; Kirby, A. J. *J. Am. Chem. Soc.* **1967**, *89*, 4853.
7. St. Pierre, T.; Jencks, W. P. *J. Am. Chem. Soc.* **1968**, *90*, 3817.
8. Williams, A. *Free Energy Relationships*; Royal Society of Chemistry: Cambridge, 2003.
9. Kirby, A. J.; Dutta-Roy, N.; da Silva, D.; Goodman, J. M.; Lima, M. F.; Roussev, C. D.; Nome, F. *J. Am. Chem. Soc.* **2005**, *127*, 7033.
10. Lipmann, F.; Tuttle, L. C. *J. Biol. Chem.* **1945**, *159*, 21.
11. Jencks, W. P. *J. Am. Chem. Soc.* **1958**, *80*, 4585.
12. Jaffe, H. H. *Chem. Rev.* **1953**, *53*, 191.
13. Broxton, T. J.; Christie, J. R.; Sango, X. *J. Org. Chem.* **1987**, *52*, 4814.
14. Fife, T. H.; Bruice, T. C. *J. Phys. Chem.* **1961**, *65*, 1079.
15. Parr, R. G.; Yang, W. *J. Chem. Phys.* **1989**, *98*, 5648.
16. Becke, A. D. *J. Chem. Phys.* **1993**, *98*, 5648.
17. Lee, C.; Yang, W.; Parr, R. G. *Phys. Rev. B* **1988**, *37*, 785.
18. Fukui, K. *Accts. Chem. Res.* **1981**, *14*, 363.
19. Peng, C.; Schlegel, H. B. *Israel J. Chem.* **1993**, *33*, 449.
20. Clark, T.; Chandrasekhar, J.; Spitznagel, G. W.; Schleyer, P. V. R. *J. J. Comp. Chem.* **1983**, *4*, 294.
21. Fukui, K. *Accts. Chem. Res.* **1981**, *14*, 363.
22. Gonzalez, C.; Schlegel, H. B. *J. Chem. Phys.* *1989*, *90*, 2154. **1989**, *90*, 2154.
23. Gonzalez, C.; Schlegel, H. B. *J. Phys. Chem.* **1990**, *94*, 5523.
24. Cossi, M.; Barone, V.; Cammi, R.; Tomasi, J. *Chem. Phys. Lett.* **1996**, *255*, 327.
25. Rappe, A. K.; Casewit, C. J.; Colwell, K. S.; Goddard, W. A.; Skiff, W. M. *J. Am. Chem. Soc.* **1992**, *114*, 10024.
26. McQuarrie, D. A. *Statistical Mechanics*; University Science Book: Sausalito CA, 2000.
27. Frisch, G. W. T., H. B. Schlegel, G. E. Scuseria, M. A. Robb, J. R. Cheeseman, J. A. Montgomery, Jr., T. Vreven, K. N. Kudin, J. C. Burant, J. M. Millam, S. S. Iyengar, J. Tomasi, V. Barone, B. Mennucci, M. Cossi, G. Scalmani, N. Rega, G. A. Petersson, H. Nakatsuji, M. Hada, M. Ehara, K. Toyota, R. Fukuda, J. Hasegawa, M. Ishida, T. Nakajima, Y. Honda, O. Kitao, H. Nakai, M. Klene, X. Li, J. E. Knox, H. P. Hratchian, J. B. Cross, C. Adamo, J. Jaramillo, R. Gomperts, R. E. Stratmann, O. Yazyev, A. J. Austin, R. Cammi, C.

Pomelli, J. W. Ochterski, P. Y. Ayala, K. Morokuma, G. A. Voth, P. Salvador, J. J. Dannenberg, V. G. Zakrzewski, S. Dapprich, A. D. Daniels, M. C. Strain, O. Farkas, D. K. Malick, A. D. Rabuck, K. Raghavachari, J. B. Foresman, J. V. Ortiz, Q. Cui, A. G. Baboul, S. Clifford, J. Cioslowski, B. B. Stefanov, G. Liu, A. Liashenko, P. Piskorz, I. Komaromi, R. L. Martin, D. J. Fox, T. Keith, M. A. Al-Laham, C. Y. Peng, A. Nanayakkara, M. Challacombe, P. M. W. Gill, B. Johnson, W. Chen, M. W. Wong, C. Gonzalez, and J. A. Pople.; Revision D.01 ed.; Gaussian Inc.: Wallingford CT, 2004.